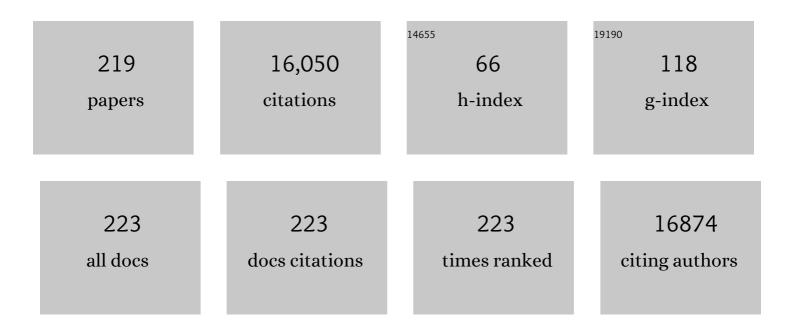
Peike Cao

List of Publications by Year in descending order

Source: https://exaly.com/author-pdf/2588575/publications.pdf Version: 2024-02-01



DEIKE CAO

#	Article	IF	CITATIONS
1	Treatment of organic wastewater by a synergic electrocatalysis process with Ti3+ self-doped TiO2 nanotube arrays electrode as both cathode and anode. Journal of Hazardous Materials, 2022, 424, 127747.	12.4	22
2	Robust ultrathin nanoporous MOF membrane with intra-crystalline defects for fast water transport. Nature Communications, 2022, 13, 266.	12.8	76
3	Electro-Fenton improving fouling mitigation and microalgae harvesting performance in a novel membrane photobioreactor. Water Research, 2022, 210, 117955.	11.3	10
4	Design Principles and Strategies of Photocatalytic H ₂ O ₂ Production from O ₂ Reduction. ACS ES&T Engineering, 2022, 2, 1068-1079.	7.6	51
5	Enhancing anaerobic methane production in integrated floating-film activated sludge system filled with novel MWCNTs-modified carriers. Chemosphere, 2022, 299, 134483.	8.2	6
6	Toxicity of biochar influenced by aging time and environmental factors. Chemosphere, 2022, 298, 134262.	8.2	14
7	Simultaneous nitrification and denitrification in continuous flow MBBR with novel surface-modified carriers. Environmental Technology (United Kingdom), 2021, 42, 3607-3617.	2.2	22
8	Electro-assisted CNTs/ceramic flat sheet ultrafiltration membrane for enhanced antifouling and separation performance. Frontiers of Environmental Science and Engineering, 2021, 15, 1.	6.0	27
9	Photocatalytic ozonation of organic pollutants in wastewater using a flowing through reactor. Journal of Hazardous Materials, 2021, 405, 124277.	12.4	24
10	Carbon-Based Materials for Electrochemical Reduction of CO ₂ to C ₂₊ Oxygenates: Recent Progress and Remaining Challenges. ACS Catalysis, 2021, 11, 2076-2097.	11.2	116
11	Highly efficient metal-free electro-Fenton degradation of organic contaminants on a bifunctional catalyst. Journal of Hazardous Materials, 2021, 416, 125859.	12.4	49
12	Alternating current-enhanced carbon nanotubes hollow fiber membranes for membrane fouling control in novel membrane bioreactors. Chemosphere, 2021, 277, 130240.	8.2	12
13	Strengthened attachment of anammox bacteria on iron-based modified carrier and its effects on anammox performance in integrated floating-film activated sludge (IFFAS) process. Science of the Total Environment, 2021, 787, 147679.	8.0	17
14	Selective reduction of nitrate to ammonium over charcoal electrode derived from natural wood. Chemosphere, 2021, 285, 131501.	8.2	16
15	Enhanced Chlorinated Pollutant Degradation by the Synergistic Effect between Dechlorination and Hydroxyl Radical Oxidation on a Bimetallic Single-Atom Catalyst. Environmental Science & Technology, 2021, 55, 14194-14203.	10.0	70
16	Durable and Selective Electrochemical H ₂ O ₂ Synthesis under a Large Current Enabled by the Cathode with Highly Hydrophobic Three-Phase Architecture. ACS Catalysis, 2021, 11, 13797-13808.	11.2	59
17	Construction of a Microchannel Aeration Cathode for Producing H ₂ O ₂ via Oxygen Reduction Reaction. ACS Applied Materials & Interfaces, 2021, 13, 56045-56053.	8.0	14
18	Performance of Alternating-Current-Enhanced Anaerobic Membrane Bioreactor: Membrane Fouling, Wastewater Treatment, and CH ₄ Production. ACS Sustainable Chemistry and Engineering, 2021, 9, 15973-15982.	6.7	8

#	Article	IF	CITATIONS
19	Selective electrochemical H2O2 generation and activation on a bifunctional catalyst for heterogeneous electro-Fenton catalysis. Journal of Hazardous Materials, 2020, 382, 121102.	12.4	137
20	Efficient electrochemical reduction of nitrobenzene by nitrogen doped porous carbon. Chemosphere, 2020, 238, 124636.	8.2	25
21	Health risk assessment of heavy metals and pesticides: A case study in the main drinking water source in Dalian, China. Chemosphere, 2020, 242, 125113.	8.2	116
22	Porous carbon membrane with enhanced selectivity and antifouling capability for water treatment under electrochemical assistance. Journal of Colloid and Interface Science, 2020, 560, 59-68.	9.4	30
23	Construction of a Microchannel Electrochemical Reactor with a Monolithic Porous-Carbon Cathode for Adsorption and Degradation of Organic Pollutants in Several Minutes of Retention Time. Environmental Science & Technology, 2020, 54, 1920-1928.	10.0	30
24	Efficient day-night photocatalysis performance of 2D/2D Ti3C2/Porous g-C3N4 nanolayers composite and its application in the degradation of organic pollutants. Chemosphere, 2020, 246, 125760.	8.2	89
25	Electrokinetic Enhancement of Water Flux and Ion Rejection through Graphene Oxide/Carbon Nanotube Membrane. Environmental Science & Technology, 2020, 54, 15433-15441.	10.0	33
26	Cross-linked Graphene Oxide Framework Membranes with Robust Nano-Channels for Enhanced Sieving Ability. Environmental Science & Technology, 2020, 54, 15442-15453.	10.0	75
27	Enhanced Photocatalytic H ₂ O ₂ Production over Carbon Nitride by Doping and Defect Engineering. ACS Catalysis, 2020, 10, 14380-14389.	11.2	265
28	High-Efficiency Electrocatalysis of Molecular Oxygen toward Hydroxyl Radicals Enabled by an Atomically Dispersed Iron Catalyst. Environmental Science & Technology, 2020, 54, 12662-12672.	10.0	114
29	Electrochemical activation of peroxymonosulfate in cathodic micro-channels for effective degradation of organic pollutants in wastewater. Journal of Hazardous Materials, 2020, 398, 122879.	12.4	31
30	Utilizing transparent and conductive SnO2 as electron mediator to enhance the photocatalytic performance of Z-scheme Si-SnO2-TiOx. Frontiers of Environmental Science and Engineering, 2020, 14, 1.	6.0	4
31	Selective electroreduction of CO2 to acetone by single copper atoms anchored on N-doped porous carbon. Nature Communications, 2020, 11, 2455.	12.8	265
32	Flexible Superhydrophobic Metal-Based Carbon Nanotube Membrane for Electrochemically Enhanced Water Treatment. Environmental Science & Technology, 2020, 54, 9074-9082.	10.0	65
33	Enhancing anaerobic digestion in anaerobic integrated floating fixed-film activated sludge (An-IFFAS) system using novel electron mediator suspended biofilm carriers. Water Research, 2020, 175, 115697.	11.3	36
34	Simultaneous nitriï¬cation and denitriï¬cation process using novel surface-modified suspended carriers for the treatment of real domestic wastewater. Chemosphere, 2020, 247, 125831.	8.2	97
35	Effects of nanomaterials on metal toxicity: Case study of graphene family on Cd. Ecotoxicology and Environmental Safety, 2020, 194, 110448.	6.0	6
36	Energy-transfer-mediated oxygen activation in carbonyl functionalized carbon nitride nanosheets for high-efficient photocatalytic water disinfection and organic pollutants degradation. Water Research, 2020, 177, 115798.	11.3	68

#	Article	IF	CITATIONS
37	Mitigating Membrane Fouling Based on In Situ •OH Generation in a Novel Electro-Fenton Membrane Bioreactor. Environmental Science & Technology, 2020, 54, 7669-7676.	10.0	43
38	Intensified degradation and mineralization of antibiotic metronidazole in photo-assisted microbial fuel cells with Mo-W catalytic cathodes under anaerobic or aerobic conditions in the presence of Fe(III). Chemical Engineering Journal, 2019, 376, 119566.	12.7	37
39	Enhanced nitrification in integrated floating fixed-film activated sludge (IFFAS) system using novel clinoptilolite composite carrier. Frontiers of Environmental Science and Engineering, 2019, 13, 1.	6.0	13
40	Novel metal-organic framework supported manganese oxides for the selective catalytic reduction of NOx with NH3: Promotional role of the support. Journal of Hazardous Materials, 2019, 380, 120800.	12.4	36
41	Effects of chlorinated polyfluoroalkyl ether sulfonate in comparison with perfluoroalkyl acids on gene profiles and stemness in human mesenchymal stem cells. Chemosphere, 2019, 237, 124402.	8.2	9
42	Vertically Aligned Janus MXene-Based Aerogels for Solar Desalination with High Efficiency and Salt Resistance. ACS Nano, 2019, 13, 13196-13207.	14.6	280
43	Efficient H2O2 generation and electro-Fenton degradation of pollutants in microchannels of oxidized monolithic-porous-carbon cathode. Water Science and Technology, 2019, 80, 970-978.	2.5	8
44	Surface water extracts impair gene profiles and differentiation in human mesenchymal stem cells. Environment International, 2019, 132, 104823.	10.0	2
45	Enhanced activation of peroxymonosulfate by CNT-TiO2 under UV-light assistance for efficient degradation of organic pollutants. Frontiers of Environmental Science and Engineering, 2019, 13, 1.	6.0	28
46	Carbon nanotubes-incorporated MIL-88B-Fe as highly efficient Fenton-like catalyst for degradation of organic pollutants. Frontiers of Environmental Science and Engineering, 2019, 13, 1.	6.0	49
47	Enhanced catalytic ozonation by highly dispersed CeO2 on carbon nanotubes for mineralization of organic pollutants. Journal of Hazardous Materials, 2019, 368, 621-629.	12.4	71
48	Enhanced heterogeneous activation of peroxymonosulfate by Co and N codoped porous carbon for degradation of organic pollutants: the synergism between Co and N. Environmental Science: Nano, 2019, 6, 399-410.	4.3	129
49	Environmentally persistent free radical generation on contaminated soil and their potential biotoxicity to luminous bacteria. Science of the Total Environment, 2019, 687, 348-354.	8.0	39
50	Performing homogeneous catalytic ozonation using heterogeneous Mn ²⁺ -bonded oxidized carbon nanotubes by self-driven pH variation induced reversible desorption and adsorption of Mn ²⁺ . Environmental Science: Nano, 2019, 6, 1932-1940.	4.3	12
51	Three-Dimensional Branched Crystal Carbon Nitride with Enhanced Intrinsic Peroxidase-Like Activity: A Hypersensitive Platform for Colorimetric Detection. ACS Applied Materials & Interfaces, 2019, 11, 17467-17474.	8.0	29
52	Comparison of CNT-PVA membrane and commercial polymeric membranes in treatment of emulsified oily wastewater. Frontiers of Environmental Science and Engineering, 2019, 13, 1.	6.0	23
53	Enhanced Perfluorooctanoic Acid Degradation by Electrochemical Activation of Sulfate Solution on B/N Codoped Diamond. Environmental Science & Technology, 2019, 53, 5195-5201.	10.0	91
54	<i>In situ</i> remediation of subsurface contamination: opportunities and challenges for nanotechnology and advanced materials. Environmental Science: Nano, 2019, 6, 1283-1302.	4.3	65

#	Article	IF	CITATIONS
55	Improvement of Antifouling and Antimicrobial Abilities on Silver–Carbon Nanotube Based Membranes under Electrochemical Assistance. Environmental Science & Technology, 2019, 53, 5292-5300.	10.0	45
56	The adverse effect of biochar to aquatic algae- the role of free radicals. Environmental Pollution, 2019, 248, 429-437.	7.5	55
57	Non enzymatic fluorometric determination of glucose by using quenchable g-C3N4 quantum dots. Mikrochimica Acta, 2019, 186, 779.	5.0	10
58	Electrochemical reduction of N ₂ to ammonia on Co single atom embedded N-doped porous carbon under ambient conditions. Journal of Materials Chemistry A, 2019, 7, 26358-26363.	10.3	51
59	Real Time Detection of Hazardous Hydroxyl Radical Using an Electrochemical Approach. ChemistrySelect, 2019, 4, 12507-12511.	1.5	14
60	Steering CO ₂ electroreduction toward ethanol production by a surface-bound Ru polypyridyl carbene catalyst on N-doped porous carbon. Proceedings of the National Academy of Sciences of the United States of America, 2019, 116, 26353-26358.	7.1	55
61	The effects of humic acid on the toxicity of graphene oxide to Scenedesmus obliquus and Daphnia magna. Science of the Total Environment, 2019, 649, 163-171.	8.0	51
62	A novel aerobic electrochemical membrane bioreactor with CNTs hollow fiber membrane by electrochemical oxidation to improve water quality and mitigate membrane fouling. Water Research, 2019, 151, 54-63.	11.3	73
63	The Technology Horizon for Photocatalytic Water Treatment: Sunrise or Sunset?. Environmental Science & Technology, 2019, 53, 2937-2947.	10.0	493
64	Development of cerium oxide-based diffusive gradients in thin films technique for in-situ measurement of dissolved inorganic arsenic in waters. Analytica Chimica Acta, 2019, 1052, 65-72.	5.4	12
65	Characterization and Formation Mechanism of the Nanodiamond Synthesized by A High Energy Arcâ€Plasma. Physica Status Solidi (A) Applications and Materials Science, 2019, 216, 1800704.	1.8	2
66	Construction of Z-Scheme g-C3N4/RGO/WO3 with in situ photoreduced graphene oxide as electron mediator for efficient photocatalytic degradation of ciprofloxacin. Chemosphere, 2019, 215, 444-453.	8.2	152
67	Improving Ion Rejection of Conductive Nanofiltration Membrane through Electrically Enhanced Surface Charge Density. Environmental Science & Technology, 2019, 53, 868-877.	10.0	83
68	Novel Anaerobic Electrochemical Membrane Bioreactor with a CNTs Hollow Fiber Membrane Cathode to Mitigate Membrane Fouling and Enhance Energy Recovery. Environmental Science & Technology, 2019, 53, 1014-1021.	10.0	71
69	A loop of catholyte effluent feeding to bioanodes for complete recovery of Sn, Fe, and Cu with simultaneous treatment of the co-present organics in microbial fuel cells. Science of the Total Environment, 2019, 651, 1698-1708.	8.0	25
70	Covalent functionalization of MoS2 nanosheets synthesized by liquid phase exfoliation to construct electrochemical sensors for Cd (II) detection. Talanta, 2018, 182, 38-48.	5.5	58
71	Efficient In Situ Utilization of Caustic for Sequential Recovery and Separation of Sn, Fe, and Cu in Microbial Fuel Cells. ChemElectroChem, 2018, 5, 1658-1669.	3.4	13
72	Deposition and separation of W and Mo from aqueous solutions with simultaneous hydrogen production in stacked bioelectrochemical systems (BESs): Impact of heavy metals W(VI)/Mo(VI) molar ratio, initial pH and electrode material. Journal of Hazardous Materials, 2018, 353, 348-359.	12.4	9

#	Article	IF	CITATIONS
73	Combined Effects of Surface Charge and Pore Size on Co-Enhanced Permeability and Ion Selectivity through RGO-OCNT Nanofiltration Membranes. Environmental Science & Technology, 2018, 52, 4827-4834.	10.0	79
74	Anti-fouling characteristic of carbon nanotubes hollow fiber membranes by filtering natural organic pollutants. Korean Journal of Chemical Engineering, 2018, 35, 964-973.	2.7	14
75	Enhanced adsorption of ionizable antibiotics on activated carbon fiber under electrochemical assistance in continuous-flow modes. Water Research, 2018, 134, 162-169.	11.3	47
76	Facile Ammonia Synthesis from Electrocatalytic N ₂ Reduction under Ambient Conditions on N-Doped Porous Carbon. ACS Catalysis, 2018, 8, 1186-1191.	11.2	520
77	Highly Permeable Thin-Film Composite Forward Osmosis Membrane Based on Carbon Nanotube Hollow Fiber Scaffold with Electrically Enhanced Fouling Resistance. Environmental Science & Technology, 2018, 52, 1444-1452.	10.0	56
78	Heterogeneous activation of peroxymonosulfate by LaCo1-xCuxO3 perovskites for degradation of organic pollutants. Journal of Hazardous Materials, 2018, 353, 401-409.	12.4	249
79	Removal of binary Cr(VI) and Cd(II) from the catholyte of MFCs and determining their fate in EAB using fluorescence probes. Bioelectrochemistry, 2018, 122, 61-68.	4.6	23
80	Enhancing nitrogen removal efficiency in a dyestuff wastewater treatment plant with the IFFAS process: the pilot-scale and full-scale studies. Water Science and Technology, 2018, 77, 70-78.	2.5	7
81	Roles of magnetite and granular activated carbon in improvement of anaerobic sludge digestion. Bioresource Technology, 2018, 249, 666-672.	9.6	163
82	Amphiphilic PA-induced three-dimensional graphene macrostructure with enhanced removal of heavy metal ions. Journal of Colloid and Interface Science, 2018, 512, 853-861.	9.4	47
83	Fluorine-doped carbon nanotubes as an efficient metal-free catalyst for destruction of organic pollutants in catalytic ozonation. Chemosphere, 2018, 190, 135-143.	8.2	75
84	Optical emission spectroscopy diagnosis of energetic Ar ions in synthesis of SiC polytypes by DC arc discharge plasma. Nano Research, 2018, 11, 1470-1481.	10.4	26
85	Effective adsorption of sulfamethoxazole, bisphenol A and methyl orange on nanoporous carbon derived from metal-organic frameworks. Journal of Environmental Sciences, 2018, 63, 250-259.	6.1	68
86	Direct growth of ultra-permeable molecularly thin porous graphene membranes for water treatment. Environmental Science: Nano, 2018, 5, 3004-3010.	4.3	5
87	Superpermeable nanoporous carbon-based catalytic membranes for electro-Fenton driven high-efficiency water treatment. Journal of Materials Chemistry A, 2018, 6, 23502-23512.	10.3	8
88	Two-dimensional nanomaterial based sensors for heavy metal ions. Mikrochimica Acta, 2018, 185, 478.	5.0	48
89	Transformation of Nitrogen and Iron Species during Nitrogen Removal from Wastewater via Feammox by Adding Ferrihydrite. ACS Sustainable Chemistry and Engineering, 2018, 6, 14394-14402.	6.7	54
90	Enhanced photocatalytic performance of a two-dimensional BiOIO3/g-C3N4 heterostructured composite with a Z-scheme configuration. Applied Catalysis B: Environmental, 2018, 237, 947-956.	20.2	99

#	Article	IF	CITATIONS
91	Photoelectrochemical aptasensor for sulfadimethoxine using g-C3N4 quantum dots modified with reduced graphene oxide. Mikrochimica Acta, 2018, 185, 345.	5.0	38
92	Stable Superhydrophobic Ceramic-Based Carbon Nanotube Composite Desalination Membranes. Nano Letters, 2018, 18, 5514-5521.	9.1	153
93	Improving the co-digestion performance of waste activated sludge and wheat straw through ratio optimization and ferroferric oxide supplementation. Bioresource Technology, 2018, 267, 591-598.	9.6	35
94	Comparing the mechanisms of ZVI and Fe3O4 for promoting waste-activated sludge digestion. Water Research, 2018, 144, 126-133.	11.3	179
95	Catalytic Ozonation in Arrayed Zinc Oxide Nanotubes as Highly Efficient Mini-Column Catalyst Reactors (MCRs): Augmentation of Hydroxyl Radical Exposure. Environmental Science & Technology, 2018, 52, 8701-8711.	10.0	45
96	Enhanced heterogeneous Fenton-like activity by Cu-doped BiFeO3 perovskite for degradation of organic pollutants. Frontiers of Environmental Science and Engineering, 2018, 12, 1.	6.0	26
97	Transcriptomic Profiles in Zebrafish Liver Permit the Discrimination of Surface Water with Pollution Gradient and Different Discharges. International Journal of Environmental Research and Public Health, 2018, 15, 1648.	2.6	9
98	Two-dimensional MoS2: A promising building block for biosensors. Biosensors and Bioelectronics, 2017, 89, 56-71.	10.1	215
99	Determination of Oxytetracycline by a Graphene—Gold Nanoparticle-Based Colorimetric Aptamer Sensor. Analytical Letters, 2017, 50, 544-553.	1.8	26
100	CO ₂ Electroreduction at Low Overpotential on Oxide-Derived Cu/Carbons Fabricated from Metal Organic Framework. ACS Applied Materials & amp; Interfaces, 2017, 9, 5302-5311.	8.0	239
101	Poly(vinylidene fluoride) hollowâ€fiber membranes containing silver/graphene oxide dope with excellent filtration performance. Journal of Applied Polymer Science, 2017, 134, .	2.6	21
102	Potentially direct interspecies electron transfer of methanogenesis for syntrophic metabolism under sulfate reducing conditions with stainless steel. Bioresource Technology, 2017, 234, 303-309.	9.6	86
103	Towards engineering application: Potential mechanism for enhancing anaerobic digestion of complex organic waste with different types of conductive materials. Water Research, 2017, 115, 266-277.	11.3	254
104	Superpermeable Atomic-Thin Graphene Membranes with High Selectivity. ACS Nano, 2017, 11, 1920-1926.	14.6	45
105	Fluorescence microscopy image-analysis (FMI) for the characterization of interphase HOË™ production originated by heterogeneous catalysis. Chemical Communications, 2017, 53, 2575-2577.	4.1	19
106	Interface evolution in the platelet-like SiC@C and SiC@SiO2 monocrystal nanocapsules. Nano Research, 2017, 10, 2644-2656.	10.4	27
107	Scaling-up of a zero valent iron packed anaerobic reactor for textile dye wastewater treatment: a potential technology for on-site upgrading and rebuilding of traditional anaerobic wastewater treatment plant. Water Science and Technology, 2017, 76, 823-831.	2.5	10
108	Is A/A/O process effective in toxicity removal? Case study with coking wastewater. Ecotoxicology and Environmental Safety, 2017, 142, 363-368.	6.0	11

Ρεικε Cao

#	Article	IF	CITATIONS
109	Photoinduced formation of reactive oxygen species and electrons from metal oxide–silica nanocomposite: An EPR spin-trapping study. Applied Surface Science, 2017, 416, 281-287.	6.1	36
110	Evaluation of the detoxification efficiencies of coking wastewater treated by combined anaerobic-anoxic-oxic (A 2 O) and advanced oxidation process. Journal of Hazardous Materials, 2017, 338, 186-193.	12.4	52
111	A colorimetric aptasensor for sulfadimethoxine detection based on peroxidase-like activity of graphene/nickel@palladium hybrids. Analytical Biochemistry, 2017, 525, 92-99.	2.4	46
112	Start-up and bacterial community compositions of partial nitrification in moving bed biofilm reactor. Applied Microbiology and Biotechnology, 2017, 101, 2563-2574.	3.6	64
113	Acute toxicity reduction and toxicity identification in pigment-contaminated wastewater during anaerobic-anoxic-oxic (A/A/O) treatment process. Chemosphere, 2017, 168, 1285-1292.	8.2	14
114	Selective Electrochemical Reduction of Carbon Dioxide to Ethanol on a Boron―and Nitrogenâ€Coâ€doped Nanodiamond. Angewandte Chemie, 2017, 129, 15813-15817.	2.0	196
115	Selective Electrochemical Reduction of Carbon Dioxide to Ethanol on a Boron―and Nitrogen oâ€doped Nanodiamond. Angewandte Chemie - International Edition, 2017, 56, 15607-15611.	13.8	226
116	New Application of Ethanol-Type Fermentation: Stimulating Methanogenic Communities with Ethanol to Perform Direct Interspecies Electron Transfer. ACS Sustainable Chemistry and Engineering, 2017, 5, 9441-9453.	6.7	41
117	Determination and prediction of octanol-air partition coefficients for organophosphate flame retardants. Ecotoxicology and Environmental Safety, 2017, 145, 283-288.	6.0	24
118	Probing the interphase "HO zone―originated by carbon nanotube during catalytic ozonation. Water Research, 2017, 122, 86-95.	11.3	72
119	Cobalt Nanoparticles Encapsulated in Porous Carbons Derived from Core–Shell ZIF67@ZIF8 as Efficient Electrocatalysts for Oxygen Evolution Reaction. ACS Applied Materials & Interfaces, 2017, 9, 28685-28694.	8.0	142
120	Innentitelbild: Selective Electrochemical Reduction of Carbon Dioxide to Ethanol on a Boron―and Nitrogenâ€Coâ€doped Nanodiamond (Angew. Chem. 49/2017). Angewandte Chemie, 2017, 129, 15678-15678.	2.0	1
121	Covering α-Fe2O3 protection layer on the surface of p-Si micropillar array for enhanced photoelectrochemical performance. Frontiers of Environmental Science and Engineering, 2017, 11, 1.	6.0	7
122	Occurrence, removal, and risk assessment of antibiotics in 12 wastewater treatment plants from Dalian, China. Environmental Science and Pollution Research, 2017, 24, 16478-16487.	5.3	96
123	Correlation between circuital current, Cu(II) reduction and cellular electron transfer in EAB isolated from Cu(II)-reduced biocathodes of microbial fuel cells. Bioelectrochemistry, 2017, 114, 1-7.	4.6	64
124	Impact of Fe(III) as an effective electron-shuttle mediator for enhanced Cr(VI) reduction in microbial fuel cells: Reduction of diffusional resistances and cathode overpotentials. Journal of Hazardous Materials, 2017, 321, 896-906.	12.4	89
125	Fluorescent probe based subcellular distribution of Cu(II) ions in living electrotrophs isolated from Cu(II)-reduced biocathodes of microbial fuel cells. Bioresource Technology, 2017, 225, 316-325.	9.6	28
126	Enhancement of anaerobic methanogenesis at a short hydraulic retention time via bioelectrochemical enrichment of hydrogenotrophic methanogens. Bioresource Technology, 2016, 218, 505-511.	9.6	66

#	Article	IF	CITATIONS
127	Enhancing nitrogen removal efficiency and reducing nitrate liquor recirculation ratio by improving simultaneous nitrification and denitrification in integrated fixed-film activated sludge (IFAS) process. Water Science and Technology, 2016, 73, 827-834.	2.5	14
128	Evaluation of the detoxication efficiencies for acrylonitrile wastewater treated by a combined anaerobic oxic-aerobic biological fluidized tank (A/O-ABFT) process: Acute toxicity and zebrafish embryo toxicity. Chemosphere, 2016, 154, 1-7.	8.2	12
129	Novel <i>in situ</i> Synthesized Fe@C Magnetic Nanocapsules Used as Adsorbent for Removal of Organic Dyes and its Recycling. Nano, 2016, 11, 1650013.	1.0	7
130	A versatile fluorescent biosensor based on target-responsive graphene oxide hydrogel for antibiotic detection. Biosensors and Bioelectronics, 2016, 83, 267-273.	10.1	123
131	Joint toxicity of cadmium and SDBS on Daphnia magna and Danio rerio. Ecotoxicology, 2016, 25, 1703-1711.	2.4	13
132	Synthesis of manganese incorporated hierarchical mesoporous silica nanosphere with fibrous morphology by facile one-pot approach for efficient catalytic ozonation. Journal of Hazardous Materials, 2016, 318, 308-318.	12.4	44
133	Communities stimulated with ethanol to perform direct interspecies electron transfer for syntrophic metabolism of propionate and butyrate. Water Research, 2016, 102, 475-484.	11.3	241
134	Electrochemical reduction of carbon dioxide to formate with Fe-C electrodes in anaerobic sludge digestion process. Water Research, 2016, 106, 339-343.	11.3	37
135	Nutrient removal performance and microbial characteristics of a full-scale IFAS-EBPR process treating municipal wastewater. Water Science and Technology, 2016, 73, 1261-1268.	2.5	26
136	Network optimization and performance evaluation of the water-use system in China's straw pulp and paper industry: a case study. Clean Technologies and Environmental Policy, 2016, 18, 257-268.	4.1	9
137	Dynamic adsorption of ciprofloxacin on carbon nanofibers: Quantitative measurement by in situ fluorescence. Journal of Water Process Engineering, 2016, 9, e14-e20.	5.6	61
138	Cooperative cathode electrode and in situ deposited copper for subsequent enhanced Cd(II) removal and hydrogen evolution in bioelectrochemical systems. Bioresource Technology, 2016, 200, 565-571.	9.6	58
139	Enhancement of sludge granulation in hydrolytic acidogenesis by denitrification. Applied Microbiology and Biotechnology, 2016, 100, 3313-3320.	3.6	14
140	A visible and label-free colorimetric sensor for miRNA-21 detection based on peroxidase-like activity of graphene/gold-nanoparticle hybrids. Analytical Methods, 2016, 8, 2005-2012.	2.7	57
141	Uncovering the Key Role of the Fermi Level of the Electron Mediator in a Z-Scheme Photocatalyst by Detecting the Charge Transfer Process of WO ₃ -metal-gC ₃ N ₄ (Metal = Cu, Ag, Au). ACS Applied Materials & Interfaces, 2016, 8, 2111-2119.	8.0	334
142	Nanocarbon-based membrane filtration integrated with electric field driving for effective membrane fouling mitigation. Water Research, 2016, 88, 285-292.	11.3	89
143	Evaluation on direct interspecies electron transfer in anaerobic sludge digestion of microbial electrolysis cell. Bioresource Technology, 2016, 200, 235-244.	9.6	157
144	Enhanced catalytic activity over MIL-100(Fe) loaded ceria catalysts for the selective catalytic reduction of NO x with NH 3 at low temperature. Journal of Hazardous Materials, 2016, 301, 512-521.	12.4	68

#	Article	IF	CITATIONS
145	Enhancing nitrogen and phosphorus removal in the BUCT–IFAS process by bypass flow strategy. Water Science and Technology, 2015, 72, 528-534.	2.5	6
146	Three-Dimensional Porous H _{<i>x</i>} TiS ₂ Nanosheet–Polyaniline Nanocomposite Electrodes for Directly Detecting Trace Cu(II) Ions. Analytical Chemistry, 2015, 87, 5605-5613.	6.5	39
147	Integration of membrane filtration and photoelectrocatalysis using a TiO2/carbon/Al2O3 membrane for enhanced water treatment. Journal of Hazardous Materials, 2015, 299, 27-34.	12.4	50
148	Monohydroxylated Polybrominated Diphenyl Ethers (OH-PBDEs) and Dihydroxylated Polybrominated Biphenyls (Di-OH-PBBs): Novel Photoproducts of 2,6-Dibromophenol. Environmental Science & Technology, 2015, 49, 14120-14128.	10.0	20
149	Fluorescent biosensor for sensitive analysis of oxytetracycline based on an indirectly labelled long-chain aptamer. RSC Advances, 2015, 5, 58895-58901.	3.6	32
150	Formation mechanism and optical characterization of polymorphic silicon nanostructures by DC arc-discharge. RSC Advances, 2015, 5, 68714-68721.	3.6	28
151	Effects of developmental perfluorooctane sulfonate exposure on spatial learning and memory ability of rats and mechanism associated with synaptic plasticity. Food and Chemical Toxicology, 2015, 76, 70-76.	3.6	54
152	An electrochemical sensor for selective determination of sulfamethoxazole in surface water using a molecularly imprinted polymer modified BDD electrode. Analytical Methods, 2015, 7, 2693-2698.	2.7	50
153	Zero-valent iron enhanced methanogenic activity in anaerobic digestion of waste activated sludge after heat and alkali pretreatment. Waste Management, 2015, 38, 297-302.	7.4	73
154	Adsorption of ciprofloxacin, bisphenol and 2-chlorophenol on electrospun carbon nanofibers: In comparison with powder activated carbon. Journal of Colloid and Interface Science, 2015, 447, 120-127.	9.4	142
155	Using three-bio-electrode reactor to enhance the activity of anammox biomass. Bioresource Technology, 2015, 196, 376-382.	9.6	46
156	Photochemical Formation of Hydroxylated Polybrominated Diphenyl Ethers (OH-PBDEs) from Polybrominated Diphenyl Ethers (PBDEs) in Aqueous Solution under Simulated Solar Light Irradiation. Environmental Science & Technology, 2015, 49, 9092-9099.	10.0	35
157	Perfluorooctane sulfonate induces apoptosis of hippocampal neurons in rat offspring associated with calcium overload. Toxicology Research, 2015, 4, 931-938.	2.1	12
158	Potential for direct interspecies electron transfer in an electric-anaerobic system to increase methane production from sludge digestion. Scientific Reports, 2015, 5, 11094.	3.3	138
159	Voltage-Gated Transport of Nanoparticles across Free-Standing All-Carbon-Nanotube-Based Hollow-Fiber Membranes. ACS Applied Materials & Interfaces, 2015, 7, 14620-14627.	8.0	14
160	High‥ield Electrosynthesis of Hydrogen Peroxide from Oxygen Reduction by Hierarchically Porous Carbon. Angewandte Chemie - International Edition, 2015, 54, 6837-6841.	13.8	419
161	Improved Photocatalytic Performance of Heterojunction by Controlling the Contact Facet: High Electron Transfer Capacity between TiO ₂ and the {110} Facet of BiVO ₄ Caused by Suitable Energy Band Alignment. Advanced Functional Materials, 2015, 25, 3074-3080.	14.9	164
162	Constructing metal-free polyimide/g-C ₃ N ₄ with high photocatalytic activity under visible light irradiation. RSC Advances, 2015, 5, 83225-83231.	3.6	28

#	Article	IF	Citations
163	Efficient Mineralization of Perfluorooctanoate by Electro-Fenton with H ₂ O ₂ Electro-generated on Hierarchically Porous Carbon. Environmental Science & Technology, 2015, 49, 13528-13533.	10.0	174
164	Efficient Electrochemical Reduction of Carbon Dioxide to Acetate on Nitrogen-Doped Nanodiamond. Journal of the American Chemical Society, 2015, 137, 11631-11636.	13.7	458
165	Enhancement of anaerobic acidogenesis by integrating an electrochemical system into an acidogenic reactor: Effect of hydraulic retention times (HRT) and role of bacteria and acidophilic methanogenic Archaea. Bioresource Technology, 2015, 179, 43-49.	9.6	40
166	Impact of dissolved organic matter on the photolysis of the ionizable antibiotic norfloxacin. Journal of Environmental Sciences, 2015, 27, 115-123.	6.1	50
167	Anaerobic biodecolorization of AO7 by a newly isolated Fe(III)-reducing bacterium <i>Sphingomonas</i> strain DJ. Journal of Chemical Technology and Biotechnology, 2015, 90, 158-165.	3.2	18
168	Biological uptake and depuration of sulfadiazine and sulfamethoxazole in common carp (Cyprinus) Tj ETQq0 0 0	rgBT/Ove	rlock 10 Tf 50
169	Electrochemiluminescence immunosensor for highly sensitive detection of 8-hydroxy-2′-deoxyguanosine based on carbon quantum dot coated Au/SiO2 core–shell nanoparticles. Talanta, 2015, 131, 379-385.	5.5	44
170	Catalytic ozonation of reactive red X-3B in aqueous solution under low pressure: decolorization and OH· generation. Frontiers of Environmental Science and Engineering, 2015, 9, 591-595.	6.0	3
171	Effective adsorption of 2,4-dichlorophenol on hydrogenated graphene: kinetics and isotherms. Science Bulletin, 2014, 59, 4752-4757.	1.7	2
172	Molecularly imprinted polymer/mesoporous carbon nanoparticles as electrode sensing material for selective detection of ofloxacin. Materials Letters, 2014, 129, 95-97.	2.6	35
173	Enhanced high-solids anaerobic digestion of waste activated sludge by the addition of scrap iron. Bioresource Technology, 2014, 159, 297-304.	9.6	138
174	Reduction of acute toxicity and genotoxicity of dye effluent using Fenton-coagulation process. Journal of Hazardous Materials, 2014, 274, 198-204.	12.4	54
175	Electrocatalytic debromination of BDE-47 at palladized graphene electrode. Frontiers of Environmental Science and Engineering, 2014, 8, 180-187.	6.0	2
176	Bioaccumulation and elimination kinetics of hydroxylated polybrominated diphenyl ethers (2′-OH-BDE68 and 4-OH-BDE90) and their distribution pattern in common carp (Cyprinus carpio). Journal of Hazardous Materials, 2014, 274, 16-23.	12.4	16
177	Ultrasensitive immunoassay of microcystins-LR using G-quadruplex DNAzyme as an electrocatalyst. International Journal of Environmental Analytical Chemistry, 2014, 94, 988-1000.	3.3	9
178	Porous metal–organic framework MIL-100(Fe) as an efficient catalyst for the selective catalytic reduction of NO _x with NH ₃ . RSC Advances, 2014, 4, 48912-48919.	3.6	80

179	A ZIF-8-based platform for the rapid and highly sensitive detection of indoor formaldehyde. RSC Advances, 2014, 4, 36444-36450.	3.6	26
180	Electrochemically enhanced adsorption of PFOA and PFOS on multiwalled carbon nanotubes in continuous flow mode. Science Bulletin, 2014, 59, 2890-2897.	1.7	17

11

#	Article	IF	CITATIONS
181	Photocatalytic Oxidation of Aqueous Ammonia Using Atomic Single Layer Graphitic-C ₃ N ₄ . Environmental Science & Technology, 2014, 48, 11984-11990.	10.0	204
182	Enhanced anaerobic fermentation with azo dye as electron acceptor: Simultaneous acceleration of organics decomposition and azo decolorization. Journal of Environmental Sciences, 2014, 26, 1970-1976.	6.1	16
183	Nitrogen-doped diamond electrode shows high performance for electrochemical reduction of nitrobenzene. Journal of Hazardous Materials, 2014, 265, 185-190.	12.4	41
184	Fabrication of atomic single layer graphitic-C3N4 and its high performance of photocatalytic disinfection under visible light irradiation. Applied Catalysis B: Environmental, 2014, 152-153, 46-50.	20.2	394
185	Photodegradation of 2,4-D induced by NO2â^' in aqueous solutions: The role of NO2. Journal of Environmental Sciences, 2014, 26, 1383-1387.	6.1	5
186	Enhanced anaerobic digestion of waste activated sludge digestion by the addition of zero valent iron. Water Research, 2014, 52, 242-250.	11.3	494
187	Electrochemical Biosensor for Detection of Perfluorooctane Sulfonate Based on Inhibition Biocatalysis of Enzymatic Fuel Cell. Electrochemistry, 2014, 82, 94-99.	1.4	22
188	Bioelectrochemical enhancement of anaerobic methanogenesis for high organic load rate wastewater treatment in a up-flow anaerobic sludge blanket (UASB) reactor. Scientific Reports, 2014, 4, 6658.	3.3	68
189	Fluorescent assay for oxytetracycline based on a long-chain aptamer assembled onto reduced graphene oxide. Mikrochimica Acta, 2013, 180, 829-835.	5.0	57
190	Cobalt implanted TiO ₂ nanocatalyst for heterogeneous activation of peroxymonosulfate. RSC Advances, 2013, 3, 520-525.	3.6	77
191	Enhancement of Catalytic Activity Over the Iron-Modified Ce/TiO ₂ Catalyst for Selective Catalytic Reduction of NO _{<i>x</i>} with Ammonia. Journal of Physical Chemistry C, 2012, 116, 25319-25327.	3.1	189
192	Graphene oxide modified g-C ₃ N ₄ hybrid with enhanced photocatalytic capability under visible light irradiation. Journal of Materials Chemistry, 2012, 22, 2721-2726.	6.7	687
193	Competitive adsorption and desorption of copper and lead in some soil of North China. Frontiers of Environmental Science and Engineering, 2012, 6, 484-492.	6.0	18
194	Photoelectrochemical immunoassay for microcystin-LR based on a fluorine-doped tin oxide glass electrode modified with a CdS-graphene composite. Mikrochimica Acta, 2012, 179, 163-170.	5.0	39
195	Cold modified microelectrode for direct tetracycline detection. Frontiers of Environmental Science and Engineering, 2012, 6, 313-319.	6.0	23
196	Enhanced photocatalytic degradation of tetracycline hydrochloride by molecular imprinted film modified TiO2 nanotubes. Science Bulletin, 2012, 57, 601-605.	1.7	30
197	TiO2 nanotube/Ag–AgBr three-component nanojunction for efficient photoconversion. Journal of Materials Chemistry, 2011, 21, 18067.	6.7	89
198	Salt-controlled assembly of stacked-graphene for capturing fluorescence and its application in chemical genotoxicity screening. Journal of Materials Chemistry, 2011, 21, 15266.	6.7	6

#	Article	IF	CITATIONS
199	Selective detection of nanomolar Cr(<scp>vi</scp>) in aqueous solution based on 1,4-dithiothreitol functionalized gold nanoparticles. Analytical Methods, 2011, 3, 343-347.	2.7	50
200	Performance of a ZVI-UASB reactor for azo dye wastewater treatment. Journal of Chemical Technology and Biotechnology, 2011, 86, 199-204.	3.2	75
201	Electrochemical Determination of Tetracycline Using Molecularly Imprinted Polymer Modified Carbon Nanotubeâ€Gold Nanoparticles Electrode. Electroanalysis, 2011, 23, 1863-1869.	2.9	77
202	Influence of Temperature and Oil Content on the Soil/Air Partition Coefficient for Hexachlorobenzene in Oil-Contaminated Rice Paddy Field Soil. Soil and Sediment Contamination, 2011, 20, 221-233.	1.9	1
203	Electrocatalytic dechlorination of 2,4,5-trichlorobiphenyl using an aligned carbon nanotubes electrode deposited with palladium nanoparticles. Science Bulletin, 2010, 55, 358-364.	1.7	8
204	Complexation of iron by salicylic acid and its effect on atrazine photodegradation in aqueous solution. Frontiers of Environmental Science and Engineering in China, 2010, 4, 157-163.	0.8	8
205	A microbial fuel cell–electroâ€oxidation system for coking wastewater treatment and bioelectricity generation. Journal of Chemical Technology and Biotechnology, 2010, 85, 621-627.	3.2	54
206	Facile fabrication, characterization, and enhanced photoelectrocatalytic degradation performance of highly oriented TiO2 nanotube arrays. Journal of Nanoparticle Research, 2009, 11, 2153-2162.	1.9	29
207	Contribution of black carbon to nonlinearity of sorption and desorption of acetochlor on sediment. Frontiers of Environmental Science and Engineering in China, 2009, 3, 69-74.	0.8	6
208	Importance of Environmental Black Carbon to Dissolved Petroleum Hydrocarbons Sorption on Soil. Soil and Sediment Contamination, 2009, 18, 184-194.	1.9	2
209	Effects of humic acid fractions with different polarities on photodegradation of 2,4-D in aqueous environments. Frontiers of Environmental Science and Engineering in China, 2008, 2, 291-296.	0.8	8
210	Toxic effect of serial perfluorosulfonic and perfluorocarboxylic acids on the membrane system of a freshwater alga measured by flow cytometry. Environmental Toxicology and Chemistry, 2008, 27, 1597-1604.	4.3	72
211	Facile Method for Fabricating Boron-Doped TiO ₂ Nanotube Array with Enhanced Photoelectrocatalytic Properties. Industrial & Engineering Chemistry Research, 2008, 47, 3804-3808.	3.7	107
212	Microwave-Induced Thermal Treatment of Petroleum Hydrocarbon-Contaminated Soil. Soil and Sediment Contamination, 2008, 17, 486-496.	1.9	10
213	Enhanced Photodegradation of PNP on Soil Surface under UV Irradiation with TiO2. Soil and Sediment Contamination, 2007, 16, 413-421.	1.9	16
214	Fabrication of nanomaterial models and their applications in water treatment. , 2007, , .		1
215	TiO ₂ â^'Multiwalled Carbon Nanotube Heterojunction Arrays and Their Charge Separation Capability. Journal of Physical Chemistry C, 2007, 111, 12987-12991.	3.1	222
216	Fabrication of needle-like ZnO nanorods arrays by a low-temperature seed-layer growth approach in solution. Applied Physics A: Materials Science and Processing, 2007, 89, 673-679.	2.3	11

#	Article	IF	CITATIONS
217	Preparation of Zn-doped TiO2 nanotubes electrode and its application in pentachlorophenol photoelectrocatalytic degradation. Science Bulletin, 2007, 52, 1456-1461.	1.7	52
218	Degradation of p-nitrophenol in aqueous solution by microwave assisted oxidation process through a granular activated carbon fixed bed. Water Research, 2006, 40, 3061-3068.	11.3	114
219	Preparation and characterization of aligned carbon nanotubes coated with titania nanoparticles. Science Bulletin, 2006, 51, 2294-2296.	1.7	14